IOP Publishing Measurement Science and Technology
Meas. Sci. Technol. **31** (2020) 045303 (18pp) https://doi.org/10.1088/1361-6501/ab4f24

An integrated measurement method for pulp consistency and pulp flow

Qiang Zhou, Xingzhi Tian, Yabo Wang, Junyu Li and Ling Tuo

School of Electrical and Control Engineering, Shaanxi University of Science and Technology, Xi'an, 710021, People's Republic of China

E-mail: 861924551@qq.com

Received 23 June 2019, revised 12 October 2019
Accepted for publication 18 October 2019
Published 16 January 2020

Abstract

An integrated method is proposed to measure pulp consistency and pulp flow, which is based on the utilization of a mechanical consistency sensor. Pulp consistency is sparsely decomposed by sparse atoms with scale properties to catch flow-velocity information in order to compute flow velocity, and then the velocity is used to compensate the consistency measured value. Sparse representation is conducted on the consistency signal by sparse atoms that have scale properties and scale-free properties, respectively, to eliminate consistency noise and obtain pulp consistency with high precision. The experimental results show that the method that only employs a consistency sensor to measure pulp consistency and pulp flow simultaneously has advantages such as high precision, strong rapidity and applicability.

Keywords: pulp consistency, pulp flow, integrated measurement, consistency noise, sparse decomposition

(Some figures may appear in colour only in the online journal)

Nomenclature

r	Radius of fiber agglomeration
R	Center distance of two adjacent fiber agglomerations
$\bar{r}$	Average of r
$\bar{R}$	Average of R
δ_r^2	Variance of r
δ_R^2	Variance of R
A	Unilateral area of the measuring knife
$d\sigma$	Unit area
f	Shear stress on the unilateral area of the measuring knife
F	Force exerted on the displacement measuring device
r_0	Arm of f with a shaft O as a fulcrum
r_1	Arm of F with a shaft O as a fulcrum
μ	Pulp dynamic viscosity
ρ	Pulp density
v	Pulp flow velocity
$\frac{\partial v}{\partial y}$	Velocity gradient within the boundary layer
f_0	Critical shearing stress exerted as pulp flows
s	Output signal of the consistency sensor
Δx	Displacement of the displacement sensor
K	Constant
c	Pulp consistency
c_0	Intercept of the pulp consistency
a	Proportional coefficient
$s(t)$	Pulp consistency signal
$\alpha(t)$	Inherent noise
$\beta(t)$	Measurement noise
$c(t)$	Consistency trend term
γ	Nonlinear coupling coefficient between $\alpha(t)$ and $\beta(t)$
$k(\cdot)$	Kurtosis
$l(\cdot)$	Skewness
$E(\cdot)$	Average of random sample
$D(\cdot)$	Variance of random sample
a_{ij}	Sparse atom's scale
$h_{a_{ij}}(t)$	Wavelet function at scale a_{ij}
j	A finite number of functions
i	A finite number of scales
M_1	Sparse atom dictionary with scale property
M_1'	Selected atom dictionary

M_2	Sparse atom dictionary with scale-free property
con_{ij}	Product constant of flow velocity v_{ij} and scale a_{ij}
$\hat{v}$	Average of the pulp flow velocity
$\alpha'(t)$	Reconstruction of consistency inherent noise $\alpha(t)$
h_a^i	ith atom in the atom dictionary M_1
sup	Supremum in the functional, i.e. the minimum upper bound
$h_{a_{ij}}^i$	Subatoms of the ith atom by selecting the former I_i scales a_{ij}
$R^i s$	Residual part conducting best match by the I_i scale of the best atom h_a^i
H	Threshold
$const_1$	Threshold of stopping sparse decomposition
S	Pipeline cross-section area
Q	Volume flow
$\Delta c(v)$	Consistency error caused by flow velocity
$\overline{c}\ (t)$	True value of pulp consistency
v_c	Pulp flow velocity under calibration state
$v(t)$	Pulp flow velocity under measurement state
$\overline{c}_c$	Consistency true value under calibration state
$\overline{c}\ (t)$	Consistency true value under measurement state
c_c	Consistency trend term under calibration state
$c(t)$	Consistency trend term under measurement state

1. Introduction

In the papermaking industries, pulp flow and pulp consistency are two physical quantities measured most frequently. The real-time and accurate measurement of pulp flow plays an important role in controlling flow, estimating absolute dry pulp and raising work efficiency in pulping and paper making sections, as well as ensuring the quality of the finished paper sheet [1]. Meanwhile, the real-time and accurate measurement of pulp consistency also has a critical effect on controlling pulp consistency accurately on the paper production line, guaranteeing pulp quality in the pulping section and improving paper quality in the papering section, as well as saving raw materials and energy consumption [2].

At present, the flow meter and consistency meter are adopted to measure pulp flow and consistency, respectively.

1.1. Current measurement methods for pulp flow

Of the various pulp flow measurement methods, electromagnetic flowmetry [3] has been widely utilized, and uses an electromagnetic flow meter as the specific application. However, this method brings some disadvantages, such as low precision, rigorous install conditions and complex electromagnetic compatible measures. Moreover, other techniques, such as pulsed ultrasonic Doppler velocimetry (PUDV) [4], nuclear magnetic resonance (NMR) [5], laser Doppler velocimetry (LDV) [6] and the correlation flow method [7], are also studied emphatically to measure pulp flow. PUDV is only suitable for moderate concentrations ($c_{mass} < 5\%$) and small pipelines ($R < 25$ mm). NMR is only used in the laboratory due to its high costs. LDV cannot be applied to industrial environments because it is susceptible to environmental noise interference. The correlation flow method applies ultrasonic signals, temperatures, image signals or pulp consistency to conduct cross-correlation analysis, whose measuring accuracy is higher than the above methods; however, the high cost limits its practical application.

In summary, a practical method with low cost and high precision is needed for measuring pulp flow in the papermaking process presently.

1.2. Current measurement methods for pulp consistency

At present, many ways to measure consistency have been used in the papermaking production, including the γ ray method [8], capacitance method [9], ultrasonic method [10], optical method [11] and mechanics method [12], of which the γ ray method, capacitance method and ultrasonic method exhibit high measuring accuracy, but their disadvantages are as follows: the cost of the γ ray method is very high, the measuring range of the capacitance method is small and the measurement result of the ultrasonic method is susceptible to bubble interference. Therefore, the mechanics method is used widely to measure pulp consistency at a moderate concentration ranging from 2% to 6% currently. The mechanics method has evolved into four types, such as external rotation, internal rotation, a stationary blade and a moving blade [12], of which the stationary blade consistency sensor is used over a wide range. But the measuring accuracy of the stationary blade consistency sensor improves slowly or remains stagnated because of flow-velocity change and consistency noise.

Hence, the current methods for pulp consistency and for pulp flow have problems such as complexity of the measuring process, high costs, low precision and poor practicality, as well as irrelevant measurements of these two physical quantities. An integrated measurement method for pulp consistency and pulp flow is proposed on the basis of a mechanical consistency sensor. Sparse decomposition [13] is used to catch flow-velocity information in the consistency signal to compute the flow velocity, and then the velocity is used to compensate the consistency measured value. And sparse representation [14] is used to eliminate consistency noise to improve the consistency measuring accuracy. Thereby, we achieve integrated measurements with high precision for pulp consistency and pulp flow.

2. Pulp consistency measurement and flow-velocity information

The basis of the suggested method is to carry out research on pulp properties and the measuring principle of the mechanical consistency sensor.

2.1. Pulp structure

Pulp is a three-phase mixture of pulp fibers, bubbles and water, which looks like floc suspended in the water [15]. Pulp

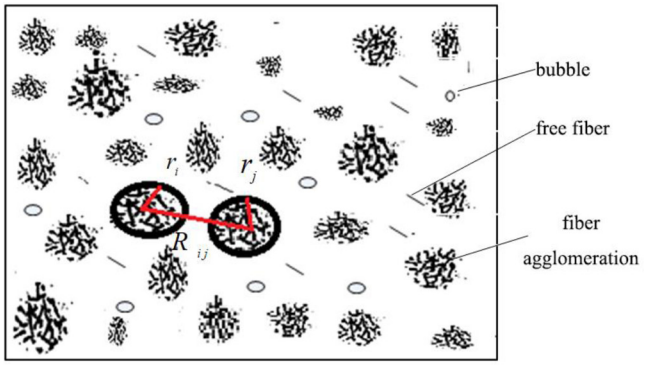

Figure 1. A schematic diagram of the pulp suspension structure.

fibers have two existence states: fiber agglomerations and free fibers. One important feature of pulp fibers is that they are often generated into fiber agglomerations called floc, which often exist in most consistency and flow conditions on the current papermaking production line. Pulp fibers are interconnected by the adhesion of hydrocarbons inside agglomerations, and they move freely and distribute randomly [16]. It is the random distribution of pulp fibers and bubbles that causes their uneven distribution. The distribution of pulp fibers is shown in figure 1. Research shows that pulp fiber morphology can be changed as the pulp state changes, such as an increase or decrease in pulp consistency and pulp flow, replacement of additives and adjustment of added content [17].

The spherical fiber agglomerations distributed randomly in water can be regarded as the physical model of pulp. The radius r of fiber agglomerations and the center distance R of two adjacent fiber agglomerations are random variables obeying some distribution laws, and they can completely reflect the morphology and the structure of pulp. Their probability models can be expressed as follows:

$$p_i(r) = \frac{1}{2\pi\sigma_{\mathrm{r}}}\mathrm{EXP}[-\frac{(r-\overline{r})^2}{2{\delta_r}^2}] \tag{2.1}$$

$$p_{ij}(R) = \frac{1}{2\pi\sigma_R}\mathrm{EXP}[-\frac{(R_{ij}-\overline{R})^2}{2{\delta_R}^2}] \tag{2.2}$$

$$\overline{r} = \frac{1}{N}\sum_{i=1}^{N} r_i \tag{2.3}$$

$$\overline{R} = \frac{1}{N\times N}\sum_{i=1}^{N}\sum_{j=1}^{N} R_{ij} \tag{2.4}$$

$$\delta_r^2 = \frac{1}{N}\sum_{i=1}^{N}(r_i-\overline{r})^2 \tag{2.5}$$

$$\delta_R^2 = \frac{1}{N\times N}\sum_{i=1}^{N}(R_{ij}-\overline{R})^2 \tag{2.6}$$

where r is the radius of the fiber agglomeration. R is the center distance of two adjacent fiber agglomerations. Here, $\overline{r}$ and $\overline{R}$ are the averages of r and R, respectively, and δ_{r}^2 and δ_{R}^2 are the variances of r and R, respectively.

Here, r and R show Gaussian distribution around their averages $\overline{r}$ and $\overline{R}$, and they also quantify the size of the fiber agglomerations and describe the morphology and the structure of the pulp fibers accurately. The parameters of $\overline{r}$, $\overline{R}$, δ_{r}^2 and δ_{R}^2 vary with pulp varieties. From equations (2.1) and (2.2), it can be found that pulp consistency must fluctuate randomly within a certain range because of the random distribution of fiber agglomerations.

2.2. Measuring principle of the mechanical consistency sensor

As shown in figure 2, the stationary blade consistency sensor is mainly composed of a sensing element (a measuring knife), a mechanical displacement system and a displacement measurement device, which works according to the mechanical equilibrium principle.

According to the fluid mechanics theory, flowing pulp, as a Bingham fluid of non-Newtonian fluid [18], will be stratified, and a laminar flow will be formed on the surface of the stationary sensing element. Then, a tangential shear stress f on the surface of the sensing element will be generated because of the viscous force caused by the interlaminar friction when the adjacent layers of fluid perform relative motion. For f to be aggregated by the measuring knife and transmitted by a lever, a force F will be formed and exerted to the displacement measuring device to cause a displacement Δx and a displacement signal s, which is the output signal of the consistency sensor.

The relationship between f and F can be built according to the conservation of angular momentum when the measurement system reaches an equilibrium state:

$$Fr_1 + 2r_0\int\int_A f d\sigma = 0 \tag{2.7}$$

where A is the unilateral area of the measuring knife; f is the shear stress on the unit area $\mathrm{d}\sigma$ of the measuring knife; F is the force exerted on the displacement measuring device; r_0 and r_1 are the arms of f and F with a shaft O as a fulcrum, respectively.

There is a definite corresponding relationship between the shear stress f, the pulp dynamic viscosity μ, the pulp density ρ and the pulp flow velocity v:

$$f = \mu\rho\frac{\partial v}{\partial y} + f_0 \tag{2.8}$$

where $\frac{\partial v}{\partial y}$ is the velocity gradient within the boundary layer, and f_0 is the critical shearing stress exerted as pulp flows.

Here, s, Δx and F show a linear relationship as follows:

$$s \propto F \propto \Delta x. \tag{2.9}$$

The non-Newtonian fluid of pulp shows the same linear characteristics as Newtonian fluid when it flows. Therefore, the relationship between s, μ, ρ and v is obtained as follows via the combined equations (2.7)–(2.9).

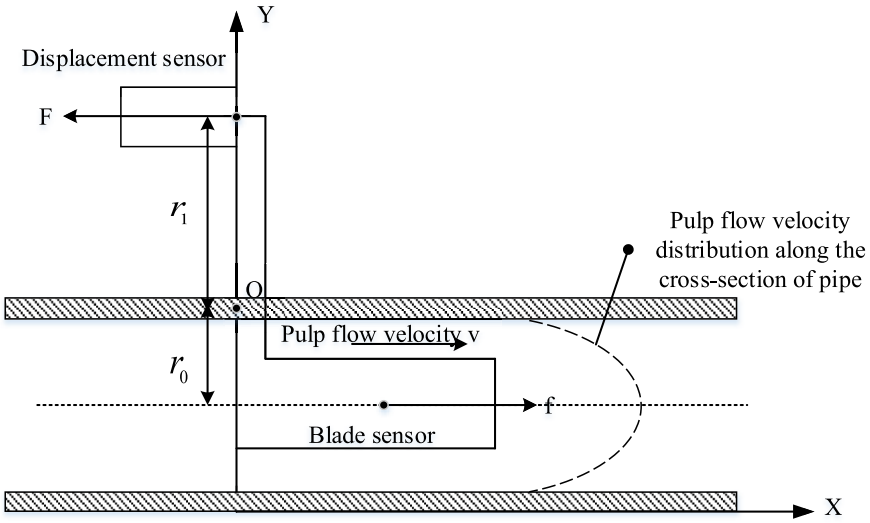

Figure 2. A schematic diagram of the principle of the stationary blade consistency sensor.

$$s = K\rho\mu v^3 \tag{2.10}$$

where K is a constant.

In a certain pulp consistency range, the pulp dynamic viscosity μ and the pulp consistency c have an approximate linear relationship:

$$\mu = ac + ac_0 \tag{2.11}$$

where c_0 is the intercept of the pulp consistency, and a is a proportional coefficient.

Substituting equation (2.11) into (2.10) on the premise that ρ is constant, the following equation can be obtained,

$$s = K'(c + c_0)v^3 \tag{2.12}$$

where

$$K' = K\rho a. \tag{2.13}$$

Equation (2.12) means that s is related to c and v.

The flow velocity in a circular pipe presents an elliptical distribution along the cross section of the pipe (as shown in figure 2), which indicates that the pulp flow velocity along the pipeline curve is the fastest, while the flow velocity near the tube wall is smaller. Hence, the velocity gradient $\frac{\partial v}{\partial y}$ formed by the pulp and the sensing element surface is the largest when the sensing element is placed along the cross section of the pipe, and the formed shear stress is the largest based on equation (2.8). The method of placing the sensing element along the pipeline curve has the best measurement effects and is often used in practice.

2.3. Compositions of the pulp consistency signal

The pulp consistency signal $s(t)$ generated by the consistency sensor contains two types of noise components. One is inherent noise $\alpha(t)$, regarded as random noise. To be precise, it is a true reflection of the uneven distribution of pulp fibers, which is caused by consistency fluctuation because the pulp consistency is high at the position of pulp fiber agglomerations and is low at the position of free fibers, water and bubbles. The other is measurement noise $\beta(t)$, independent of pulp properties, which is caused by the vibration of the mechanical consistency sensor and the thermal noise of electronic components in the circuits.

With the exception of the random noise components, the other part in $s(t)$ can be expressed by a function $c(t)$ called the consistency trend term, which contains the true value of the consistency. It is easy to find that $s(t)$ is composed by $c(t)$, $\alpha(t)$ and $\beta(t)$, not in a simple addition. A previous study [7] shows that the two noises in pulp consistency are coupled linearly and nonlinearly, respectively, and are also coupled to the trend term with an additive mode, thus the pulp consistency can be expressed as

$$s(t) = c(t) + \alpha(t) + \beta(t) + \gamma\alpha(t)\beta(t) \tag{2.14}$$

where γ is the nonlinear coupling coefficient between $\alpha(t)$ and $\beta(t)$.

In general, $\alpha(t)$ is larger in amplitude that is entirely dependent on the structure of pulp fibers, while the amplitude of $\beta(t)$ is only dependent on the performance of the consistency sensor. The higher the precision grade of the sensor, the smaller the amplitude of $\beta(t)$. But $\beta(t)$ could not be completely eliminated. Hence, it is difficult to obtain the actual consistency $c(t)$ from the consistency signal $s(t)$.

2.4. Noise properties of the pulp consistency signal

The inherent noise $\alpha(t)$ and measurement noise $\beta(t)$ do not have the same properties. Traditional de-noising methods cannot achieve satisfactory results by using low-pass filters to eliminate consistency noises blindly under an unknown consistency noise property conditions [19]. Therefore, it is necessary to study consistency noise properties.

2.4.1. Gaussian properties of pulp consistency noise. It is a prerequisite to determine the analysis and processing method that establishes whether the noise signal obeys Gaussian distribution, because the current de-noising methods are unable to process non-Gaussian noise.

Here, we adopt a high-order statistics method to confirm the Gaussian properties of pulp consistency noise. And the conclusion can be drawn that $\alpha(t)$ obeys Gaussian distribution while $\beta(t)$ obeys non-Gaussian distribution by carrying out the fourth-order statistics kurtosis and the third order statistics skewness to $\alpha(t)$ and $\beta(t)$, respectively [20]. Obviously, it inevitably causes a large error in signal processing if we assume that $\beta(t)$ is Gaussian white noise:

$$k_\alpha = E\left[\frac{\alpha(t) - E(\alpha(t))^4}{\sqrt{D(\alpha(t))}}\right] - 3 \tag{2.15}$$

$$k_\beta = E\left[\frac{\beta(t) - E(\beta(t))^4}{\sqrt{D(\beta(t))}}\right] - 3 \tag{2.16}$$

$$l_\alpha = E\left[\frac{\alpha(t) - E(\alpha(t))^3}{\sqrt{D(\alpha(t))}}\right] \tag{2.17}$$

$$l_\beta = E\left[\frac{\beta(t) - E(\beta(t))^3}{\sqrt{D(\beta(t))}}\right] \tag{2.18}$$

where $k_{(\cdot)}$ is the kurtosis, $l_{(\cdot)}$ is the skewness, $E(\cdot)$ is the average of the random sample and $D(\cdot)$ is the variance of the random sample.

2.4.2. Stationary random properties of pulp consistency noise. The stationary random process [19], a statistical property of a stochastic process that does not vary with time, determines whether the signal is analyzed in the frequency domain or the time–frequency domain. The non-stationary random signals are usually processed with time–frequency analysis. Here, $\alpha(t)$ and $\beta(t)$ are time-varying in the power spectrum density (PSD). Therefore, they are non-stationary signals in a strict sense.

However, the non-stationary random property of these two noises is different. The noise $\alpha(t)$ is a colored noise with a weak time-varying mathematical model [21]. Thus it can be approximated as a stationary random process in a short time, while $\beta(t)$ is much closer to non-stationary white noise because of its strong time-varying mathematical model and wide frequency bandwidth. Therefore, it cannot be regarded as a stationary random process at short notice.

2.4.3. Velocity-scale characteristics of pulp consistency noise. Velocity-scale characteristics [22] are a property that describes the telescopic transformation of a noise curve as the pulp flow velocity changes. To be specific, the rapid fluctuation of noise, high frequency and curve compression can be observed by the consistency sensor when the pulp flows quickly; while the slow fluctuation of noise, low frequency and curve extension can also be observed when the pulp flows slowly.

As a true reflection of the inhomogeneity of the pulp fiber structure, $\alpha(t)$ represents a certain velocity characteristic, despite its singularity and randomness. A phenomenon is found in the study that $\alpha(t)$ has flow-velocity characteristics while $\beta(t)$ does not because it is irrelevant to the pulp flow velocity.

2.5. Velocity information in pulp consistency noise

The corresponding relationship between the pulp flow velocity and noise scale, which is the velocity information hidden in the consistency noise, can be found by conducting quantitative analysis of the flow-velocity characteristics of pulp consistency noise. Then, we can compute the flow velocity. The quantitative relationship of velocity-scale characteristics is as follows:

The consistency signal will vary from $s(t)$ to $s(kt)$ if the pulp flow velocity varies from v to v/k (k is a positive real number), and we can see that $c(t)$ and $\alpha(t)$ have a corresponding scale variation, but $\beta(t)$, which is irrelevant to the flow velocity, does not:

$$\begin{aligned} s(kt) &= c(kt) + \alpha(kt) + \beta(t) + \gamma\alpha(kt)\beta(t) \\ &= c(kt) + \alpha(kt)(1 + \gamma\beta(t)) + \beta(t). \end{aligned} \tag{2.19}$$

But the scale variation of $c(kt)$ cannot be observed in most functional spaces due to its large scale. The mean $\bar{\beta}$ of $\beta(t)$ can be obtained via the statistical calculation. Let $1 + \gamma\bar{\beta} = \beta'$. We have

$$\begin{aligned} s(kt) &= c(kt) + \alpha(kt)(1 + \gamma\bar{\beta}) + \beta(t) \\ &\approx c(kt) + \beta\prime\alpha(kt) + \beta(t). \end{aligned} \tag{2.20}$$

Hence, $\alpha(kt)$ scaled with the flow velocity change can be observed in a functional space. Decompose and reconstruct $\alpha(t)$ in the wavelet space:

$$\alpha(t) \approx \sum_{i=1}^{\infty} \langle s(t), h_{a_i}(t)\rangle h_{a_i}(t) \tag{2.21}$$

where $h_{a_i}(t)$ is a wavelet function at the scale a_i, and its scale can be used as a characteristic quantity to reflect the flow velocity change,

$$\begin{aligned} \alpha(kt) \approx \sum_{i=1}^{\infty} \langle s(kt), h_{a_i}(kt)\rangle h_{a_i}(kt) = \sum_{i=1}^{\infty} \langle s(kt), h_{ka_i}(t)\rangle h_{ka_i}(t) \\ \underline{\underline{a_i' = ka_i}} \sum_{i=1}^{\infty} \langle s(kt), h_{a_i'}(t)\rangle h_{a_i'}(t). \end{aligned} \tag{2.22}$$

Here, $\alpha(t)$ is difficult to fit by a finite number of single wavelet functions $h_{a_i}(t)$ that show the poor sparsity due to the strong and high dimension of inherent noise; therefore, a large number of wavelet functions are needed, even $i \to \infty$, and then a large computation will be brought [17]. Here, we use the diversity of a sparse atom dictionary to fit inherent noise $\alpha(t)$, i.e. to conduct sparse decomposition to $\alpha(t)$ in the atom dictionary that is easy to extract scale characteristics,

$$\alpha(t) \approx \sum_{j=1}^{J} \sum_{i=1}^{I} \langle s(t), h_{a_{ji}}^{j}(t)\rangle h_{a_{ji}}^{j}(t). \tag{2.23}$$

In equation (2.23), $h^j_{a_{ji}}(t)$ represents the function of the jth atom at scale a_{ji}, where j and i ($j = 1,2,\ldots$ J, $i = 1,2\ldots$I) represent a finite number of functions and scales, respectively. Here, $\alpha(t)$ can be expressed by sparse atoms when its scale varies with the flow velocity change,

$$\alpha(kt) \approx \sum_{j=1}^{J}\sum_{i=1}^{I}\langle s(kt), h^j_{a_{ji}}(kt)\rangle h^j_{a_{ji}}(kt) = \sum_{j=1}^{J}\sum_{i=1}^{I}\langle s(kt), h^j_{ka_{ji}}(t)\rangle h^j_{ka_{ji}}(t)$$
$$\underline{\underline{a'_{ji} = ka_{ji}}} \sum_{j=1}^{J}\sum_{i=1}^{I}\langle s(kt), h^j_{a'_{ji}}(t)\rangle h^j_{a'_{ji}}(t). \tag{2.24}$$

Multiple scales of different sparse atoms can reflect the change in flow velocity, hence these scales are chosen as the characteristic quantities of pulp flow velocity.

It can be deduced from equation (2.24) that flow information hidden in the consistency inherent noise can be extracted if we choose scale a_{ji} as the characteristic quantity. When the pulp flow velocity varies from v to $v/k(= v')$, the consistency signal will change from $s(t)$ to $s(kt)$, the inherent noise will change from $\alpha(t)$ to $\alpha(kt)$ and the function scales in the sparse atom dictionary will change from a_{ji} to $a'_{ji}(= ka_{ji})$. It is clear in equation (2.25) that the product of the pulp flow velocity and the function scales in the sparse atom dictionary are constant. Therefore, there is an inverse relation between the flow velocity v and the function scales a_{ji},

$$v' \cdot a' = (v/k)\cdot(ka_{ji}) = v \cdot a_{ji} = con_{ij} \tag{2.25}$$

$$v \propto 1/a_{ji} \quad (j = 1,2,\cdots,J, i = 1,2,\cdots,I). \tag{2.26}$$

We can observe that the atom scale a_{ji}, chosen as the characteristic quantities, can accurately reflect the flow velocity hidden in the consistency noise.

It is the differences in properties between $\alpha(t)$ and $\beta(t)$ that make us unable to use the same method to separate them from $c(t)$. Based on the property that sparse decomposition can establish the basis functions flexibly by different objects, we establish two types of over-complete atom dictionaries [23] that have scale properties and scale-free properties, respectively, to carry out sparse decomposition and sparse representation of the two types of noises, and then separate the two types of noises from the consistency signal and separate them from each other effectively.

3. Integrated measurement for pulp consistency and pulp flow

3.1. Thought and process of integrated measurement for pulp consistency and pulp flow

3.1.1. Thought of integrated measurement for pulp consistency and pulp flow. The thought of the integrated measurement method for pulp consistency and pulp flow is proposed for the following reasons: the pulp consistency signal generated by the consistency sensor contains flow velocity information, and consistency noise and pulp flow velocity are the main obstacles to improving the measuring accuracy of the consistency sensor.

(1) The flow-velocity information contained in the pulp consistency signal is used to achieve soft measurement for the pulp flow;
(2) The noise component is separated and eliminated from the pulp consistency signal;
(3) The velocity compensation of the pulp consistency measured value is carried out by the flow velocity computed by step (1).

3.1.2. Process of integrated measurement for pulp consistency and pulp flow. The process of integrated measurement for pulp consistency and pulp flow is shown in figure 3.

Step A: pulp consistency is measured by the mechanical consistency sensor to obtain the original consistency signal, which contains the true value of the pulp consistency, the consistency error caused by flow velocity and the inherent noise, as well as the measurement noise;
Step B: the inherent noise in the pulp consistency signal is identified, reconstructed and separated. Considering that the inherent noise contains flow-velocity information, it will be further processed in step C. In step E, the consistency signal filtering out the inherent noise will be processed because it also contains the true value of the pulp consistency, the consistency error caused by flow velocity and the measurement noise;
Step C: the inherent noise of the pulp consistency is analyzed by the random signal process to extract characteristic quantities that reflect the flow-velocity information, which is on the basis that the flow-velocity information is hidden in a batch of characteristic quantities of consistency inherent noise. The obtained characteristic quantities are used in step D;
Step D: the characteristic quantities of pulp flow obtained from step C are computed by the soft measurement algorithm to acquire the real-time flow velocity, which is the flow velocity measured value of the integrated measurement method proposed in this paper. Moreover, the computed flow velocity can also be used in the flow-velocity compensation in step F;
Step E: the measurement noise in the pulp consistency signal without inherent noise is identified, reconstructed and separated. It can be directly eliminated as it does not contain any useful information. The residual signal contains the true value of the pulp consistency and the consistency error caused by flow velocity now, which will be processed in step F;
Step F: the compensation of the flow-velocity error is conducted by the flow-velocity information obtained in step D in accordance with the flow-velocity compensation formula of the pulp consistency, and then the flow-velocity error can be eliminated to acquire the true value of the pulp consistency that is called the consistency measured value in the paper.

The integrated measurement employing the consistency sensor to measure pulp consistency and pulp flow can be

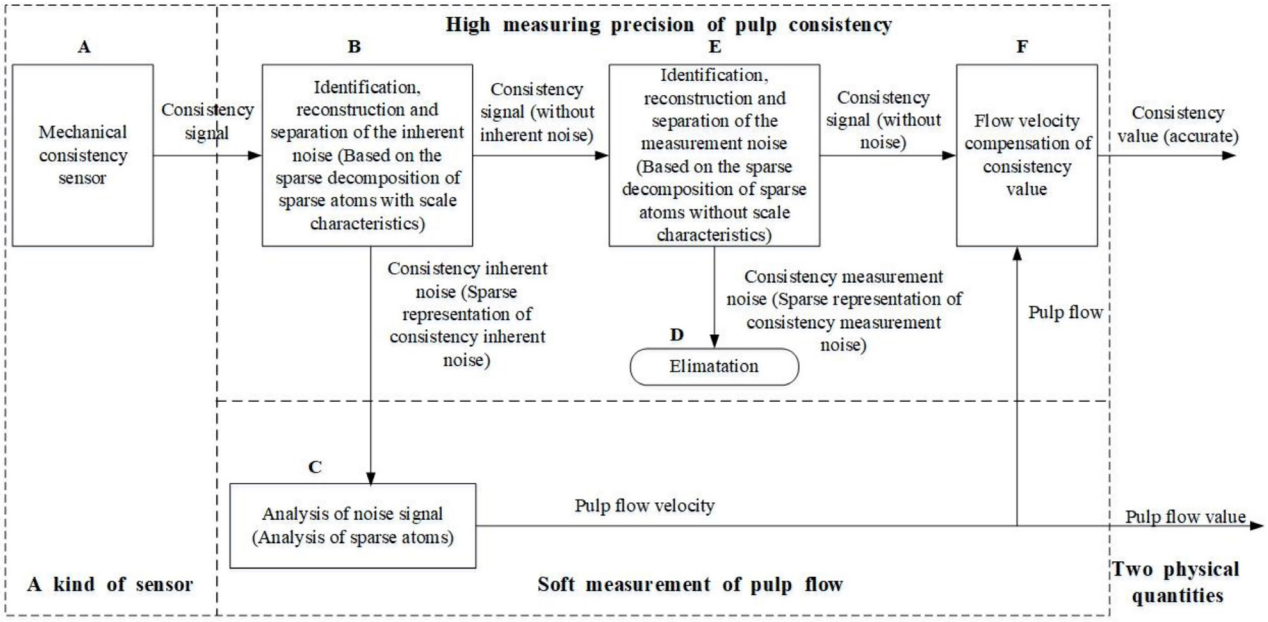

Figure 3. The process of the pulp consistency–flow integrated measurement.

achieved by the above steps. Compared with the traditional consistency measurement, it can not only obtain the accurate pulp flow velocity, but can also improve the consistency measured value significantly.

3.2. Soft measurement for pulp flow based on sparse decomposition

The integrated measurement for pulp consistency and pulp flow depends on the analysis and utilization of consistency noise. Since sparse decomposition has the feature whereby its basis functions are flexible in order to preserve the main characteristics of the signals and reduce the signal processing cost when signals are decomposed in the over-complete atom dictionary, it is thus chosen as the analysis method for consistency noise.

3.2.1. Process of soft measurement of pulp flow. The complete process for soft measurement of pulp flow can be seen in figure 4.

(1) Sparse decomposition based on the sparse atom dictionary with scale properties.
Sparse decomposition is conducted on the pulp consistency signal $s(t)$ by the atoms from the sparse atom dictionary M_1 with scale properties. At the same time, a batch of sparse atoms of different scales (including the same kind of sparse atoms at different scales) are constructed and put into the selected atom dictionary M_1'.

(2) Extraction for characteristic quantities of pulp flow.
It can be deduced from section 2.5 that each sparse atom's scale a_{ij} in the atom dictionary M_1' contains flow-velocity information. The scale a_{ij} can be regarded as the characteristic quantity of pulp flow velocity according to the inverse relation between the flow velocity and the scale, and then each atom $h^i_{a_{ij}}$ in the atom dictionary M_1' can provide the flow-velocity characteristic quantity a_{ij}.

(3) Calculation for pulp flow velocity based on the sparse atom's scale.
The inverse relation between the flow velocity v_{ij} and the sparse atom's scale a_{ij} is utilized to calibrate the product constant con_{ij} of v_{ij} and a_{ij}. The corresponding flow velocity v_{ij} can be computed by the sparse atom's scale a_{ij} obtained from the pulp consistency signal in real-time. And then the flow velocity $\widehat{v}$ can finally be acquired by averaging the flow velocity calculated from all sparse atoms.

(4) Besides, the sparse representation of the sparse atom's function $h^i_{a_{ij}}(t)$ and the sparse coefficient $\langle s(t), h^i_{a_{ij}}(t)\rangle$ can realize the reconstruction of the consistency inherent noise, denoted by $\alpha'(t)$, which will be applied in pulp consistency de-noising in section 3.3.2.

3.2.2. Establishment of sparse atom dictionary and sparse decomposition with scale properties.

(1) Establishment of two sparse atom dictionaries
The velocity-scale property is the biggest difference between the two types of noises discussed in section 2.4, thus the atom dictionary $M1$ with the scale property and the atom dictionary $M2$ with the scale-free property are established, respectively. The atom dictionary $M1$ mainly includes the basis functions whose scale characteristics are clear and easy to extract, such as the Gauss function, Morlet function and Meyer function [24]; while the functions in the atom dictionary $M2$ are the impulse function, Daubechies function system, biorthogonal (biorNr. Nd) function system, Coiflet (coifN) function system,

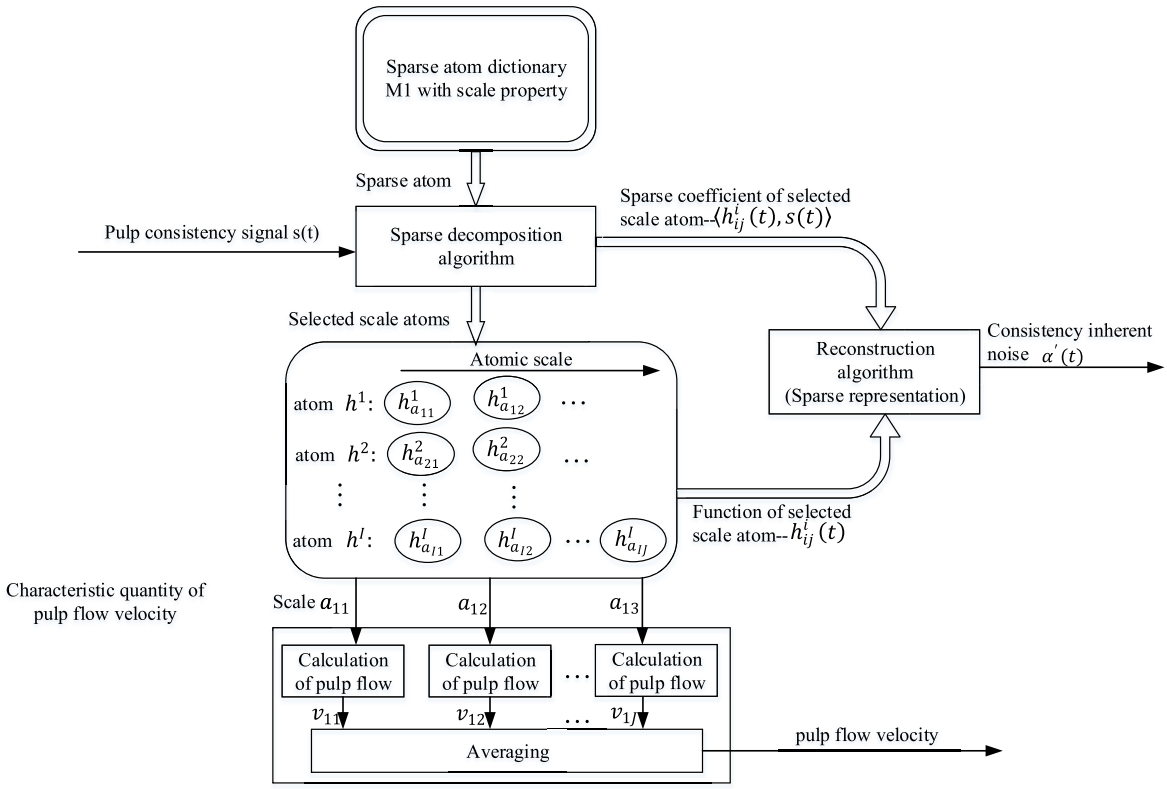

Figure 4. The process for soft measurement of pulp flow based on sparse decomposition.

Symlets(symN) function system and other functions, whose scale characteristics are unclear and difficult to extract [25].

(2) Sparse decomposition with scale properties
The sparse decomposition of consistency inherent noise is obtained by analyzing the consistency signal using sparse atoms in the atom dictionary $M1$. Meanwhile, the flow velocity is computed via the scale factors of sparse atoms.

Sparse decomposition is conducted on the consistency signal $s(t)$ by using the atom h_a^l in the atom dictionary $M1 = \{h_a^l \,|l = 1, 2, \cdots L\}$ that has scale properties. The first atom h_a^1 is confirmed via the following equation:

$$\left|\left\langle s(t), h_a^1\right\rangle\right| = \sup_{j,a\in\tau}\left|\sum_{i=1}^{I}\left\langle s(t), h_{a_{li}}^{l}\right\rangle\right| \tag{3.1}$$

where *sup* is the supremum in the functional, i.e. the minimum upper bound. The atom h_a^l in the atom dictionary $M1$ best matched to $s(t)$ is selected via *sup*. Here, h_a^1 is the first atom selected in the process, and its scales are a_{1i} $(i = 1, 2, 3, \cdots, I_1)$, which are sorted by the sizes of the different scales $\left|\left\langle s(t), h_{a_{1i}}^{1}\right\rangle\right|$,

$$\left|\left\langle s(t), h_{a_{11}}^{1}\right\rangle\right| > \left|\left\langle s(t), h_{a_{12}}^{1}\right\rangle\right| > \cdots > \left|\left\langle s(t), h_{a_{1I}}^{1}\right\rangle\right| > \cdots . \tag{3.2}$$

The subatoms h_{a11}^1, h_{a12}^1, …, h_{a1I}^1 of the first atom are constructed by selecting the former I_1 scales $a_{11}, a_{12}, \ldots, a_{1I_1}$, whose amplitudes $\left|\left\langle s(t), h_{a_{1i}}^{1}\right\rangle\right|$ are greater than a certain threshold H, and then conduct the best match on the consistency signal s,

$$s = \sum_{i=1}^{I_1}\left\langle s(t), h_{a_{1i}}^{1}\right\rangle h_{a_{1i}}^{1} + R^1 s \tag{3.3}$$

where $R^1 s$ is the residual part conducting the best match by the I_1 scale of the best atom h_a^1, and we continue to do sparse decomposition to $R^1 s$. The second atom h_a^2 is confirmed via the following equation,

$$\left|\left\langle R^1 s, h_a^2\right\rangle\right| = \sup_{j,a\in\tau}\left|\sum_{i=1}^{I}\left\langle R^1 s, h_{a_{li}}^{l}\right\rangle\right|. \tag{3.4}$$

The subatoms h_{a21}^2, h_{a22}^2, …, h_{a2I}^2 of the second atom are constructed by selecting the former I_2 scales a_{21}, a_{22}, …, a_{2I_2}, whose amplitudes $\left|\left\langle R^1 s, h_{a_{2i}}^{2}\right\rangle\right|$ are greater than a certain threshold H, and then conduct the best match on the consistency residual signal $R^1 s$,

$$s = \sum_{i=1}^{I_1}\left\langle A_1, h_{a_{1i}}^{1}\right\rangle h_{a_{1i}}^{1} + \sum_{i=1}^{I_2}\left\langle R^1 s, h_{a_{2i}}^{2}\right\rangle h_{a_{2i}}^{2} + R^2 s \tag{3.5}$$

where $R^2 s$ is the residual part conducting the best match to the consistency residual signal $R^1 s$ by the best atom h_a^2 , and we continue to carry out sparse decomposition until the Jth atom h_a^J, and its subatoms $h_{a_{J1}}^J$, $h_{a_{J2}}^J$, …, $h_{a_{JI_J}}^J$ at the scales of a_{J1}, a_{J2},

…, a_{JI_J} are constructed to carry out the best match to the consistency signal $R^{J-1}s$:

$$s = \sum_{i=1}^{I_1} \left\langle s(t), h^1_{a_{1i}} \right\rangle h^1_{a_{1i}} + \sum_{i=1}^{I_2} \left\langle R^1 s, h^2_{a_{2i}} \right\rangle h^2_{a_{2i}} + \cdots + \sum_{i=1}^{I_J} \left\langle R^{J-1} s, h^J_{a_{Ji}} \right\rangle h^J_{a_{Ji}} + R^J s. \tag{3.6}$$

When it meets the condition

$$\sum_{i=1}^{I_J} \left\langle R^{J-1} s, h^J_{a_{Ji}} \right\rangle < const_1 \tag{3.7}$$

stops sparse decomposition. In equation (3.7), $const_1$ is the threshold of stopping sparse decomposition. Let $R^0 s = s(t)$; we have

$$s = \sum_{j=0}^{J-1} \sum_{i=1}^{I_J} \left\langle A_1, h^j_{a_{1i}} \right\rangle h^j_{a_{1i}} + R^J s. \tag{3.8}$$

In general, the number of sparse atom varieties and scales depends on the singularity of the consistency inherent noise. The more complex the noise is, the more sparse atom varieties and scales are needed to fit it. H and $const_1$ are both determined empirically. Partial flow-velocity information will be lost if the two thresholds are too big, while if they are too small, some measurement noise will be introduced.

3.2.3. Calculation of pulp flow velocity. A complete calculation process of pulp flow velocity contains calibration and flow velocity calculations.

(1) Calibration
Here, v' is recorded when the pulp flow velocity v is stable. Meanwhile, the function scales a_{11}, a_{12}, …, a_{JI_J} of the various sparse subatoms $h^1_{a_{11}}$, $h^1_{a_{12}}$, …, $h^J_{a_{JI_J}}$ are extracted and recorded as a^b_{11}, a^b_{12},…, $a^b_{JI_J}$. The products $con_{11}(= a^b_{11}v')$, $con_{12}(= a^b_{12}v')$, …, $con_{JI_J}(= a^b_{JI_J}v')$ of v' and a^b_{11}, a^b_{12},…, $a^b_{JI_J}$ are calculated and recorded.

(2) Flow velocity calculation
The function scales a_{11}, a_{12}, …, a_{JI_J} of the various sparse subatoms $h^1_{a_{11}}$, $h^1_{a_{12}}$, …, $h^1_{a_{12}}$ are extracted when the flow velocity v is stable in the measuring state.

These scales are the reflection of pulp flow velocity by various sparse subatoms. In equation (2.26), the flow velocity and the function scales represent an inverse relation, so they satisfy the following equations, respectively,

$$a^b_{11}v' = a_{11}v_{11} = con_{11} \tag{3.9}$$

$$a^b_{12}v' = a_{12}v_{12} = con_{12} \tag{3.10}$$

$$a^b_{JI_J}v' = a_{JI_J}v_{JI_J} = con_{JI_J}. \tag{3.11}$$

Convert them to

$$v_{11} = \frac{a^b_{11}v'}{a_{11}} = \frac{con_{11}}{a_{11}} \tag{3.12}$$

$$v_{12} = \frac{a^b_{12}v'}{a_{12}} = \frac{con_{12}}{a_{12}} \tag{3.13}$$

$$v_{JI_J} = \frac{a^b_{JI_J}v'}{a_{JI_J}} = \frac{con_{JI_J}}{a_{JI_J}}. \tag{3.14}$$

Then, we can obtain the current flow velocity by executing the mean to the flow velocity v_{11}, v_{12}, …, v_{JI_J} computed by the scales a_{11}, a_{12}, …, a_{JI_J} of various subatoms,

$$\widehat{v} = \sum_{j=0}^{J-1} \sum_{i=1}^{I_J} v_{ji}. \tag{3.15}$$

Consequently, this method has high measuring accuracy because the flow velocity is computed by the multiple scales of multiple atoms.

In the meantime, the current pulp volume flow can be obtained by multiplying the pulp flow velocity $\hat{v}$ by the pipeline cross-section area S,

$$Q = \hat{v}S. \tag{3.16}$$

The pulp flow velocity $\hat{v}$ and volume flow Q have different applications, respectively.

3.3. Method for improving measuring accuracy of pulp consistency

3.3.1. Influencing factors and improving scheme for the measuring accuracy of the consistency sensor.

(1) Factors affecting the measuring accuracy of the consistency sensor
There are mainly two factors that affect the measuring accuracy of the consistency sensor according to the theory in section 2.
One is the influence of noises in the pulp consistency signal. The output signal $s(t)$ contains inherent noise and measurement noise, as well as their nonlinear coupling via equation (2.14). And the noise components are difficult to eliminate using the traditional filtering methods due to their different properties. The other is the consistency error caused by the flow velocity. It is known from equation (2.12) that the flow-velocity change brings the consistency error $\Delta c(v)$ to the consistency true value $\overline{c}(t)$; therefore, the consistency trend term $c(t)$ in equation (2.14) is composed of the consistency true value $\overline{c}(t)$ and the consistency error $\Delta c(v)$:

$$c(t) = \overline{c}(t) + \Delta c(v). \tag{3.17}$$

Hence, the measured value of the pulp consistency in equation (2.14) can be re-expressed as

$$s(t) = \overline{c}(t) + \Delta c(v) + \alpha(t) + \beta(t) + \gamma\alpha(t)\beta(t). \tag{3.18}$$

(2) Scheme for improving the measuring accuracy of pulp consistency
It is consistency noises and flow velocity that influence the measuring accuracy of the consistency sensor. Thus, it is necessary to filter out the consistency noises $\alpha(t)$ and $\beta(t)$ in equation (3.18). Meanwhile, the flow-velocity

compensation for the consistency trend term, based on the accurate measurement of flow velocity, should be done to eliminate $\Delta c(v)$ and preserve $\bar{c}(t)$.

The proposed scheme is carried out as follows. Here, $\alpha(t)$ and $\beta(t)$ are eliminated, respectively, by means of sparse representation at first. Then, the velocity compensation is conducted on pulp consistency using the flow velocity obtained by soft measurement according to the velocity compensation equation of pulp consistency.

3.3.2. Method for eliminating consistency noises based on sparse representation.

(1) Elimination of consistency inherent noise.
The product coupling term $\gamma\alpha(t)\beta(t)$ is too weak to be considered, compared to the measurement noise and the inherent noise.
Sparse representation is conducted on $\alpha(t)$ by the sparse decomposition result of $\alpha(t)$ in the atom dictionary $M1$:

$$\alpha'(t) = \sum_{j=0}^{J-1}\sum_{i=1}^{I_J} \langle A_1, h^j_{a_{1i}}\rangle h^j_{a_{1i}}. \tag{3.19}$$

The inherent noise from the consistency signal $s(t)$ is eliminated using the sparse representation $\alpha\prime(t)$ of the consistency inherent noise:

$$\begin{aligned} R^J s &= s(t) - \alpha'(t) = \bar{c}(t) + \Delta c(v) + \alpha(t) + \beta(t) \\ &\quad - \alpha'(t) \approx \bar{c}(t) + \Delta c(v) + \beta(t). \end{aligned} \tag{3.20}$$

(2) Elimination of consistency measurement noise.
Sparse decomposition is carried out on the residual consistency signal $R^J s$ using the atoms in the atom dictionary $M2$ that has the scale property.

The first atom in the atom dictionary $M2$ is selected by the following equation:

$$\left|\left\langle R^J s, y_j\right\rangle\right| = \sup_{j,a\in\tau} \left|\left\langle R^J s, y_j\right\rangle\right| \tag{3.21}$$

here, y_1 is the selected atom in this process,

$$R^J s = \left\langle R^J s, y_1\right\rangle y_1 + R^1 s' \tag{3.22}$$

where $R^1 s'$ is the residual part conducting the best match to the consistency residual signal $R^J s$ by the best atom y_1, and we continue to carry out sparse decomposition to obtain the sparse atoms y_2, y_3, …, y_K and obtain the best match to $R^J s$. When it meets the condition,

$$\left\langle R^{K-1} s, y_K\right\rangle < const_2 \tag{3.23}$$

stops sparse decomposition. Here, $const_2$ is the threshold of stopping sparse decomposition.

Then, we obtain

$$R^J s = \sum_{k=1}^{K} \left\langle R^J s, y_k\right\rangle y_k + R^K s'. \tag{3.24}$$

Conduct sparse representation to $\beta(t)$ using the sparse decomposition result,

$$\beta'(t) = \sum_{k=1}^{K} \left\langle R^J s, y_k\right\rangle y_k. \tag{3.25}$$

Eliminate the measurement noise in the residual term $R^J s$,

$$R^K s' = R^J s - \beta'(t) \approx \bar{c}(t) + \Delta c(v) = c(t). \tag{3.26}$$

It can be clearly seen that the residual term $R^K s'$ only contains the consistency trend term $\bar{c}(t)$ and the consistency error $\Delta c(v)$ caused by flow velocity. Therefore, velocity compensation should be carried out to compensate the influence of flow velocity change.

3.3.3. Velocity compensation for the pulp consistency measured value

(1) Establishing the velocity compensation equation for pulp consistency.
The velocity compensation equation for pulp consistency is established using equation (2.12). Assuming the pulp flow velocities are v_c and $v(t)$, the true values of the pulp consistency are $\bar{c}_c$ and $\bar{c}(t)$, and the consistency trend terms are c_c and $c(t)$, when the integrated measurement system is in the calibration state and measurement state, respectively. After they are substituted to equation (2.12), we have

$$c_c = K'(\bar{c}_c + c_0)v_c^3 \tag{3.27}$$

$$c(t) = K'(\bar{c}(t) + c_0)^{\frac{1}{2}} v^3(t). \tag{3.28}$$

Equation (3.27) is divided by equation (3.28), which can be obtained by derivation:

$$\bar{c}(t) = \frac{(\bar{c}_c + c_0)v_c^3}{c_c v^3(t)} c(t) - c_0 = \frac{(\bar{c}_c + c_0)v_c^3}{c_c v^3(t)} (c(t) + \Delta c(v)) - c_0. \tag{3.29}$$

Equation (3.29) is what we call the velocity compensation equation for pulp consistency measurement, where v_c, $\bar{c}_c$ and c_c are the fixed values obtained by calibration. Here, $v(t)$ is obtained by means of soft measurement, and $c(t)(=\bar{c}(t) + \Delta c(v))$ containing the error term $\Delta c(v)$ can be obtained by eliminating $\alpha(t)$ and $\beta(t)$ from the consistency measured value (seen in equations (3.19)–(3.26)). After substituting v_c, $\bar{c}_c$, c_c and $v(t)$ into equation (3.29), we obtain the consistency true value $\bar{c}(t)$ eliminated error $\Delta c(v)$. The detailed process is as follows.

(2) Calibrating velocity compensation equation.
The consistency measured value c_c (de-noising), consistency true value $\bar{c}_c$ and flow true value v_c are substituted into equation (3.29) when the flow velocity is constant, and let

$$K'' = \frac{(\bar{c}_c + c_0)v_c^3}{c_c} \tag{3.30}$$

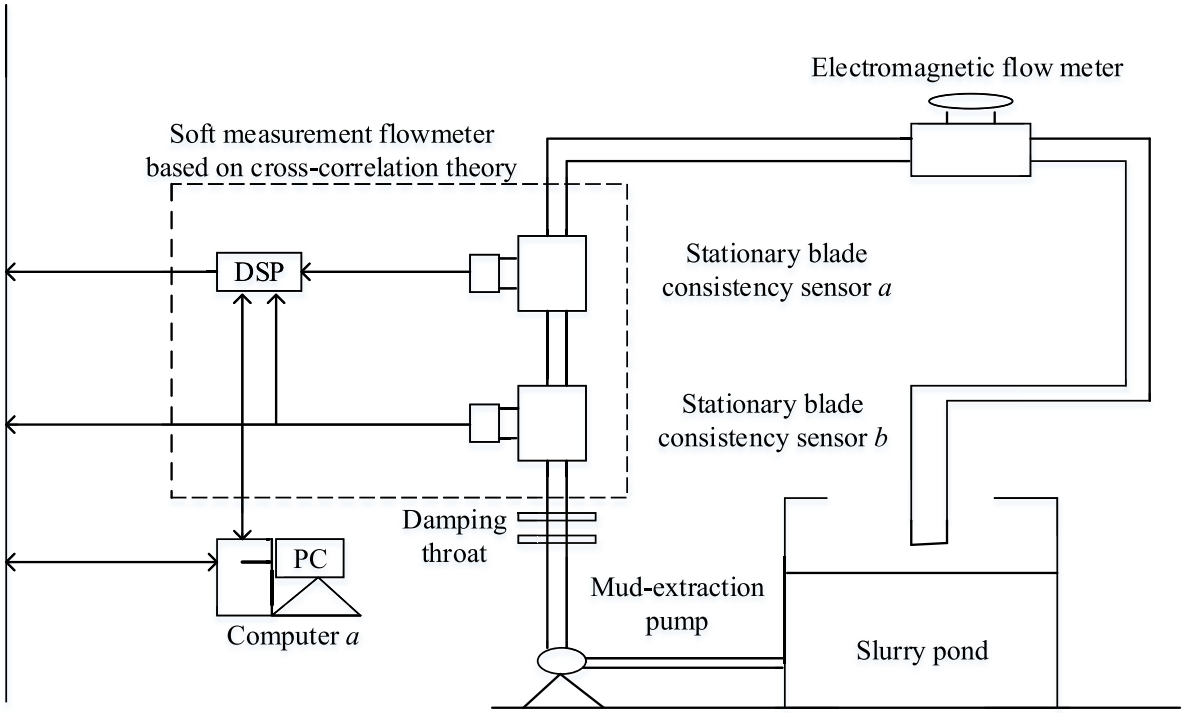

Figure 5. The experimental system.

where c_0 is the known pulp consistency intercept. Then, we have

$$\bar{c}(t) = \frac{K''}{v^3(t)}c(t) - c_0. \tag{3.31}$$

Record c_0 and K''.

(3) Compensating flow velocity.
Here, $\widehat{v}$ in equation (3.15) is the accurate estimate value of $v(t)$, i.e. $\widehat{v} \approx v(t)$, and $R^K s'$ in equation (3.26) is the accurate estimate value of $c(t)$, i.e. $R^K s' \approx c(t)$. Therefore, equation (3.31) can be re-expressed as

$$\bar{c}(t) = \frac{K''}{\hat{v}^3}R^K s' - c_0. \tag{3.32}$$

Substitute the flow velocity $\hat{v}$ calculated by equation (3.15) and the consistency value $R^K s'$ calculated by equation (2.10) into (3.32), and the pulp consistency with high measuring accuracy is obtained.

3.3.4. Feasibility analysis for improving measuring accuracy of pulp consistency. A complete measured value contains a true value, a systematic error and a random error in accordance with the measuring principle. The results show that in the measured value generated by the mechanical consistency sensor, the inherent noise $\alpha(t)$ and the measurement noise $\beta(t)$ are random errors, and $\Delta c(v)$ is the main component of the systematic error. Here, 0.5% fluctuations in the pulp flow velocity will result in 1.5% absolute error in the pulp consistency measured value.

(1) Feasibility analysis for eliminating random errors
The inherent noise and the measurement noise are non-stationary random signals which cannot be filtered out by the traditional filtering methods, but can be filtered out through identification, reconstruction and separation. The key aim is to carry out accurate matching to these two noises with different properties.
Aiming at the scale property of the inherent noise and the singularity of the measurement noise, two types of sparse atom dictionaries are established utilizing the characteristics whereby the sparse decomposition can construct the basis function flexibly based on different objects, thereby achieving accurate matching to these two noises and eliminating the random error in the consistency measured value effectively.

(2) Feasibility analysis for eliminating systematic errors
As $\Delta c(v)$ is a function $\Delta c(v(t))$ with the pulp flow velocity $v(t)$ as an independent variable, therefore, the key to eliminating systematic error is to offset $\Delta c(v)$ with a real-time and accurate flow velocity value $\widehat{v}(t)$.

The soft measurement method for pulp flow velocity has high precision and good real-time performance, which ensures the successful compensation of $\Delta c(v)$ during the accurate measurement of pulp consistency, and then totally eliminates the systematic error in the pulp consistency measured value.

4. Validation experiment

4.1. Experimental conditions

4.1.1. Experimental system. The experimental system adopted to verify the suggested method is shown in figure 5, which is composed of a slurry pond, a mud extracting pump, pipelines

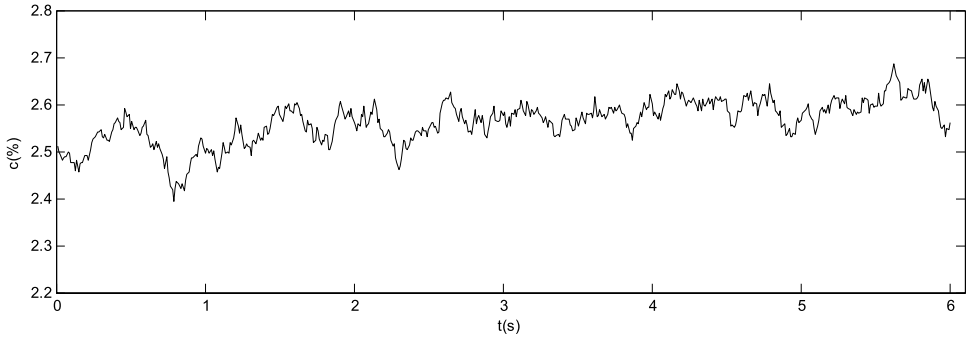

Figure 6. The original pulp consistency curve.

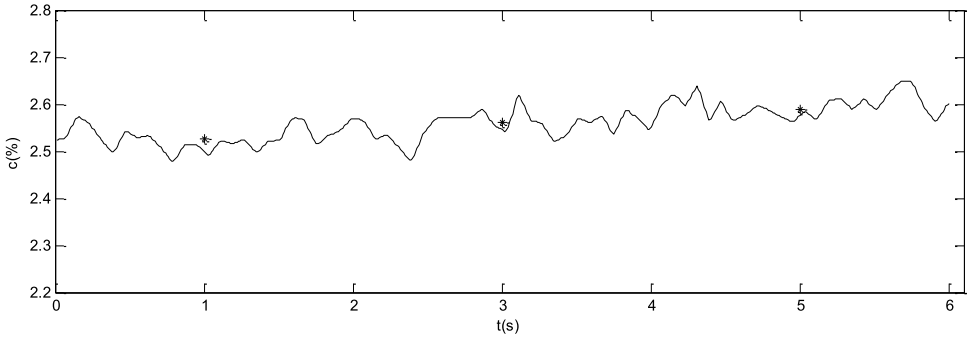

(a)

(‘*’is the true value obtained by assay)

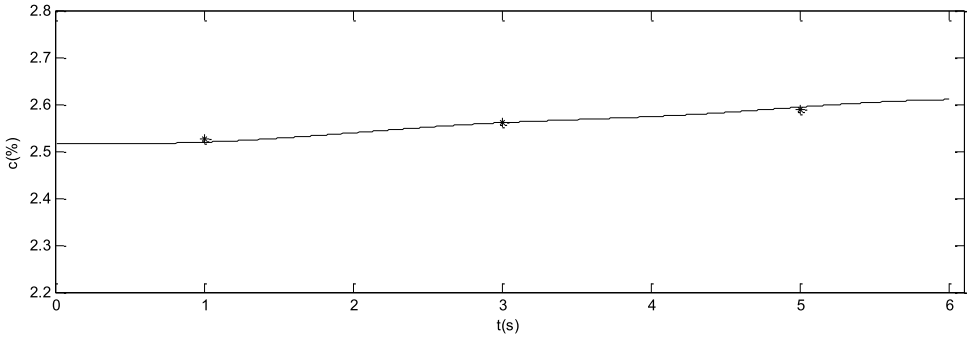

(b)

Figure 7. Improving the measuring accuracy of pulp consistency using wavelet transform and EMD. (a) The three-level Morlet wavelet packet decomposition method (‘∗’is the true value obtained by assay). (b) The four-layer EMD decomposition method.

and instruments installed on the pipelines, forming a pulp circulation system. Two sets of stationary blade consistency sensors (XDBN-1000), with the measuring range of 1.2% ~3.6% and the measuring accuracy of 1.0% are installed in the circulation system. A set of electromagnetic flow meter (ADMAGAE) with the measuring accuracy of 1.0% is also installed in the experimental system. In addition, computer *a* is used to process the data, and compute the pulp consistency and the pulp flow.

4.1.2. Method for obtaining the standard physical quantities. The standard pulp consistency value and the standard pulp flow value are the necessary physical quantities to test the measuring accuracy of the suggested method.

(a) The standard pulp consistency value is obtained by means of an assay carried out by the laboratory technician. The pulp consistency is calculated accurately by steps involving collecting pulp samples at the production site, and then performing slurry separation and drying, dehydration and weighing of the dry pulp to a unit volume of pulp in the laboratory.
(b) The standard pulp flow value is provided by a cross-correlation measurement method, which can obtain the pulp flow velocity with high measuring accuracy by

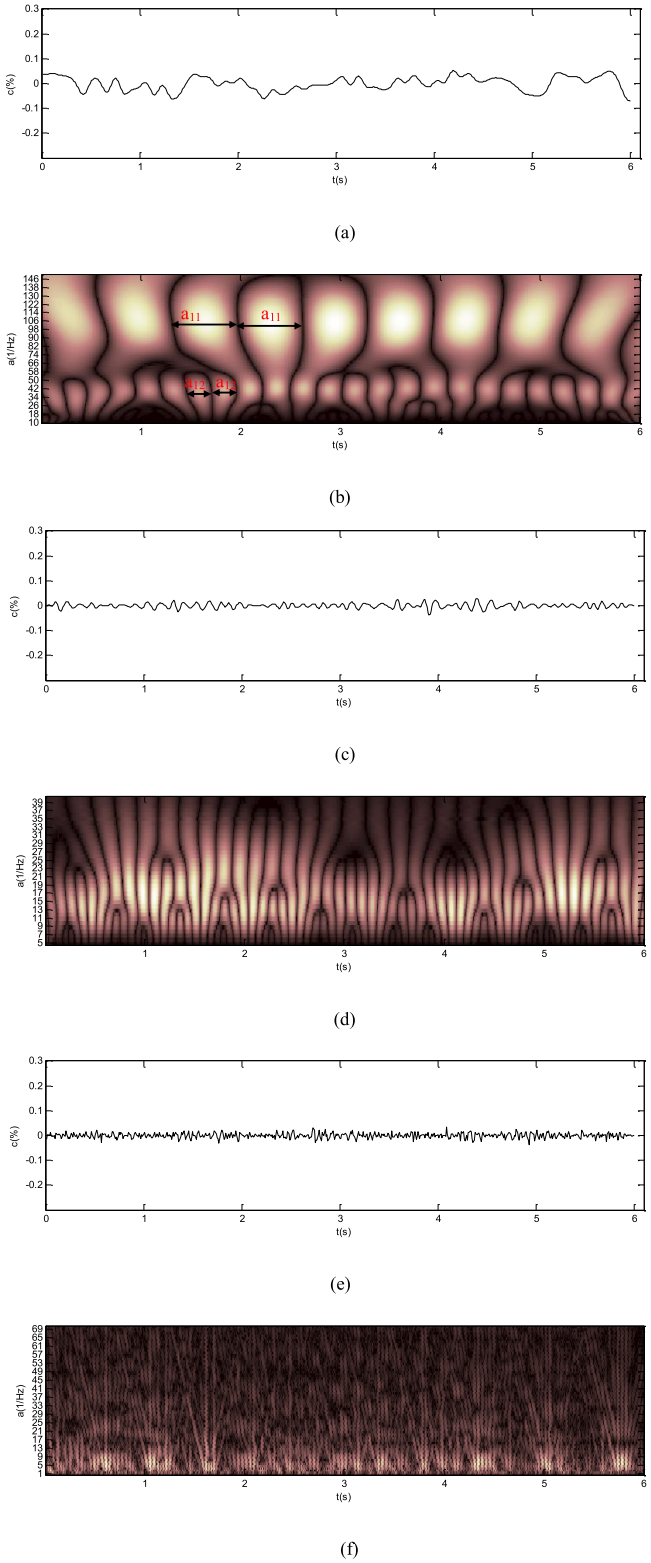

Figure 8. The process of acquiring characteristic scales by analyzing the pulp consistency signal using various sparse atoms (corresponding to $\hat{v} = 2.09$ m s^{-1}). (a) Consistency noise reconstruction of the multiscale Morlet atom. (b) Scale analysis of the Morlet reconstructed atom. (c) Consistency noise reconstruction of the multiscale Gauss atom. (d) Scale analysis of Gauss reconstructed atoms. (e) Consistency noise reconstruction of the multiscale db2 atom. (f) Scale analysis of the db2 reconstructed atom.

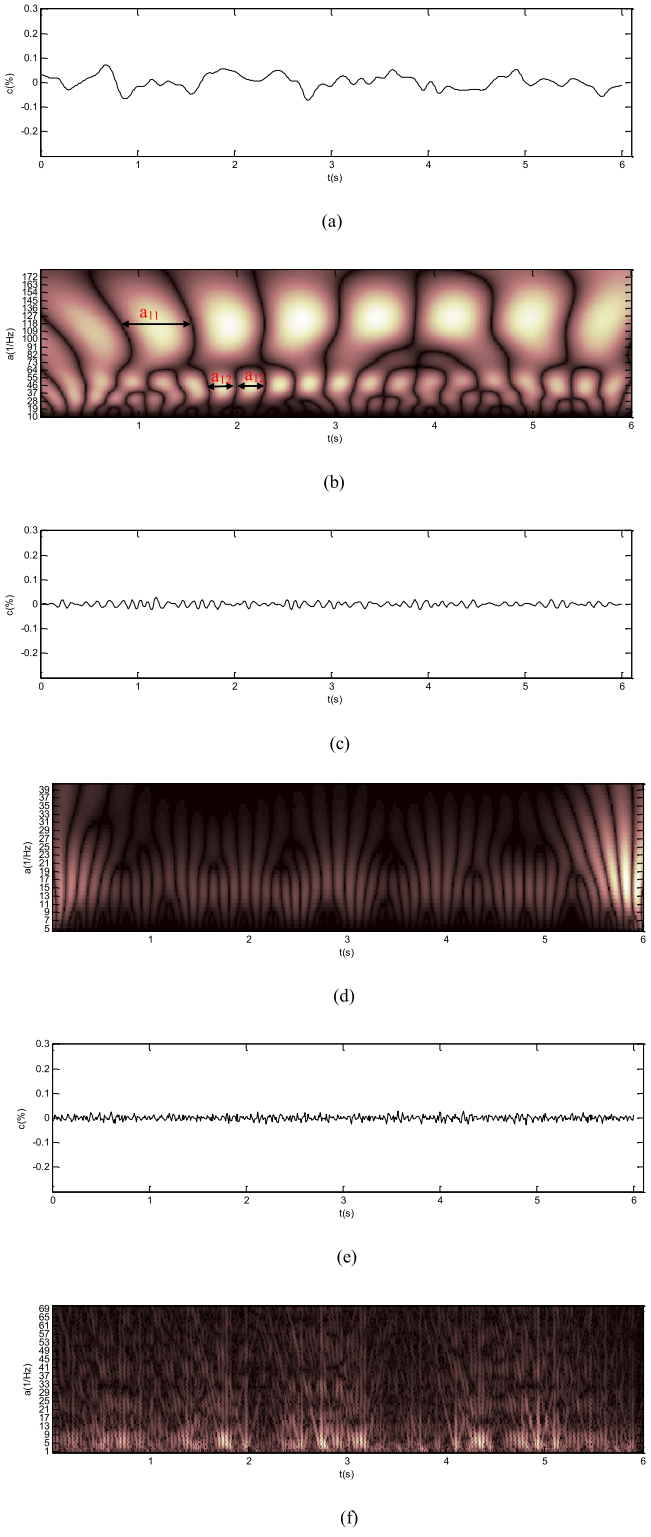

Figure 9. The process of acquiring characteristic scales by analyzing the pulp consistency signal using various sparse atoms (corresponding to $\hat{v} = 1.78$ m s^{-1}). (a) Consistency noise reconstruction of the multiscale Morlet atom. (b) Scale analysis of the Morlet reconstructed atom. (c) Consistency noise reconstruction of the Gauss atom. (d) Scale analysis of the Gauss reconstructed atom. (e) Consistency noise reconstruction of the multiscale db2 atom. (f) Scale analysis of the db2 reconstructed atom.

conducting cross-correlation analysis of the consistency signal on a flow measurement system consisting of two consistency sensors. The measuring accuracy reaches 0.02%, so the measured value can be regarded as the standard flow value. The working principle and the specific operation are shown in [12].

4.2. Feasibility experiment of the suggested method

4.2.1. Experimental process.

(1) Record the standard flow value and the standard consistency value, as well as the current consistency curve when the flow is stable, as shown in figure 6.
We use wavelet transform and empirical mode decomposition (EMD) to eliminate consistency noise. The curve shown in figure 7(a) is the consistency trend term that removes high-frequency components by conducting the three-level Morlet wavelet packet decomposition of the original consistency signal. And figure 7(b) shows the consistency trend term by carrying out the four-layer EMD decomposition of the original consistency signal. The measuring accuracies of the pulp consistency by means of these two methods are 0.46% and 0.37%, respectively, in the case of the flow-velocity change.

(2) Conduct sparse decomposition of the original consistency signal using the sparse atom dictionary that has scale properties.
The pulp consistency signal is sparsely decomposed to obtain sparse atoms with characteristic scales, such as the Morlet atom, Gauss atom and db2 atom with characteristic scales via equations (3.1) and (3.8). Scale analysis using two scales of Morlet atoms and three scales of Gauss atoms are shown in figures 8(a)–(f), and the scale unit is second.
From the spectra of figures 8(b), (d) and (f), we can obtain the scales of the sparse atoms directly. Taking figure 8(b) as an example, it is clear to see the two scales' regions of the Morlet atom. The region with 70–145 (1/Hz) as an ordinate and 0–6 (S) as an abscissa is the forming region of the large scale atom a_{11} of the Morlet atom, while the region with 35–50 (1/Hz) as an ordinate and 0–6 (S) as an abscissa is the forming region of the small scale atom a_{12} of the Morlet atom. The two a_{11} shown in the figure are the large scale values of the Morlet atom at $t = 2$ S, while the two a_{12} are the small scale values at $t = 2$ S. It can be concluded from table 1 that the average of the large scale is about 0.6860 S at $t = 2$ S, and the average of the small scale is about 0.2564 S. Figures 9(a)–(f) are the scale analyses for the pulp consistency signal at the other flow velocity using the same method.
For example, the two scales' regions of the Morlet atom are also seen clearly in figure 9(b). It can be concluded from table 1 that the value of a_{11} is about 0.8055 S at $t = 2$ S, and the average of a_{12} is about 0.3018S. By comparing figure 8(b) with 9(b), we find that as the flow velocity decreases, the longitudinal fringe distance of the spectrum increases and these are scale increases. The products of the flow velocity and the large scale are 1.433 74 and 1.433 79, while the products of the flow velocity and the small scale are 0.535 876 and 0.537 204, which are computed at the flow velocities $\hat{v} = 2.09$ m s^{-1} and $\hat{v} = 1.78$ m s^{-1}, respectively. The results are approximately equal, which verifies the conclusion that the products of the flow velocity and scales are approximately constant in equation (2.25) in section 2.5, i.e. the flow velocity is inverse to the scale.

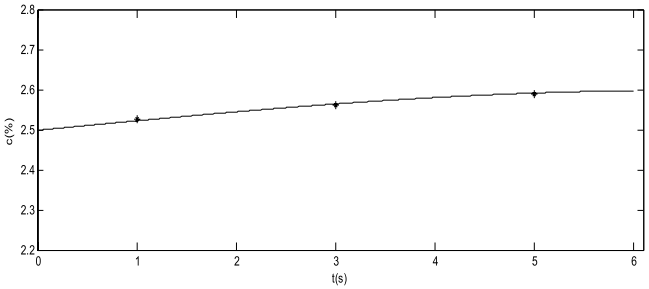

Figure 10. The pulp consistency curve after de-noising.

(3) Calculating pulp flow velocity via characteristic scales of sparse atoms.
Calibration: this should be finished before the formal measurement. Record the current characteristic scales a_{11}^b, a_{12}^b, ..., $a_{JI_J}^b$ when the flow velocity is stable at $v' = 1.78$ m s^{-1}. Then, calculate the products of these scales and the flow velocity, and preserve the results as calibration values. For example, con_{11}(=1.433 79) is the product of the Morlet atom scale $a_{11} = 0.8055$ and $v' = 1.78$ m s^{-}1, while con_{12}(=0.537 204) is the product of the Morlet atom scale $a_{12} = 0.3018$ and $v' = 1.78$ m s^{-1}.
Calculation: calculate the current flow velocity using the current characteristic scales a_{11}, a_{12}, …, a_{JI_J} and their corresponding calibration values, according to equations (3.12) and (3.14).

(4) Pulp consistency de-noising.
The inherent noise in the pulp consistency signal can be eliminated via equations (3.19) and (3.20). The measurement noise is sparsely decomposed via equations (3.21)–(3.25) and eliminated via equation (3.26). The pulp consistency curve after de-noising is shown in figure 10.

(5) Velocity compensation for the pulp consistency measured value.
The flow-velocity measured value $\hat{v}$ is used to conduct velocity compensation of the pulp consistency measured value to obtain the pulp consistency $\bar{c}(t)$ via equation (3.29).

4.2.2. Experimental results.

(1) Measuring accuracy of the suggested method
Table 2 shows the consistency measuring accuracy obtained by means of EMD de-noising, wavelet trans-

Table 1. Sparse scales obtained at different flow velocities (corresponding to $v' = 1.78$ m s^{-1} and $\hat{v} = 2.09$ m s^{-1}).

Pulp flow velocity (m s^{-1})	Atom type	Atom scale (s)	Time (S)					
			1	2	3	4	5	…
2.09	Morlet	a1	0.6857	0.686	0.6855	0.6862	0.6859	…
		a2	0.2571	0.2564	0.2579	0.2588	0.2582	…
	Gauss	g1	0.2028	0.2035	0.2024	0.2041	0.2039	…
		g2	0.1159	0.1163	0.1152	0.115	0.1157	…
		g3	0.0724	0.0711	0.0729	0.0736	0.0725	…
1.78	Morlet	a1	0.8052	0.8055	0.8049	0.8053	0.8046	…
		a2	0.3031	0.3038	0.3018	0.3025	0.3027	…
	Gauss	g1	0.2393	0.2396	0.238	0.2386	0.2377	…
		g2	0.1358	0.135	0.1365	0.1359	0.1353	…
		g3	0.0851	0.0844	0.0849	0.0842	0.0857	…
…	…	…	…	…	…	…	…	…

Table 2. A comparison of the pulp consistency measuring accuracy.

Measurement indicator	EMD de-noising	Wavelet transform de-noising	The suggested method
Maximum absolute error	0.0093	0.0118	0.0064
Maximum relative error	0.37	0.46	0.25
average error ± mean square deviation	0.0083 ± 0.0003	0.0112 ± 0.0004	0.0043 ± 0.0001

form de-noising and the suggested method. It can be seen by comparison that the suggested method is better than the EMD de-noising method and the wavelet transform de-noising method with regards to the maximum absolute error and the maximum relative error, which presents the highest measuring accuracy.

From table 3, the measuring accuracy of the soft measurement method for pulp flow is higher than the electromagnetic flow meter. Meanwhile, the measuring accuracy of the suggested method and electromagnetic flow meter is decreased accompanied by the decrease in the flow velocity.

(2) Real-time performance of the suggested method

The experiment shows that the suggested method demonstrates a good real-time performance. The maximum lag time for measuring pulp consistency is within 0.05 s, and for measuring pulp flow is within 0.2 s, which can satisfy the rapidity requirements in the practical production process.

(3) Experimental conclusion

(a) The flow measurement method proposed in this paper has a higher measuring accuracy than other measurement methods, and its cost is zero compared with various flow meters whose costs are commonly higher.

(b) The measurement method for pulp consistency, based on the mechanical consistency sensor, improves the measuring accuracy of pulp consistency from 1% to 0.25%; thus it is a high-precision method for measuring pulp consistency.

(c) The experiment proves that the suggested method is basically feasible, and the applicability will be further verified in this paper.

4.3. Applicability experiment

We also change the experimental conditions to verify the applicability of the proposed measurement method, and then confirm its feasibility sufficiently.

4.3.1. Control of experimental conditions. Various experimental states are necessary to verify the applicability (or robustness) of the suggested method. The following conditions are considered in the experimental system.

(1) Change in pulp types. Various pulps are provided, for example, mechanical wood pulp, sulphate bamboo pulp, wastepaper pulp and so on.

(2) Change in pulp consistency. The pulp consistency ranging from 1.5% to 4% is obtained by diluting pulp in a slurry pond.

(3) Change in pulp flow. The pulp flow ranging from 0 m s^{-1} to 4.5 m s^{-1} is obtained by regulating the power of the mud-extraction pump.

(4) Control of noise in the pulp consistency. Non-stationary white noise with an amplitude of 0–10 times of the measurement noise $\beta(t)$ is directly added to the consistency signal in computer a, for the purpose of verifying the noise sensitivity of the suggested method.

4.3.2. Experimental results. The applicability of the suggested method for pulp consistency, pulp flow and noise signal are shown in figure 11, in the case of the substantial change in external conditions. Furthermore, the performances of traditional methods, including the pulp consistency measurement method based on wavelet de-noising and the pulp flow measurement method based on an electromagnetic flow meter, are also plotted in figure 11 for comparison with the suggested method.

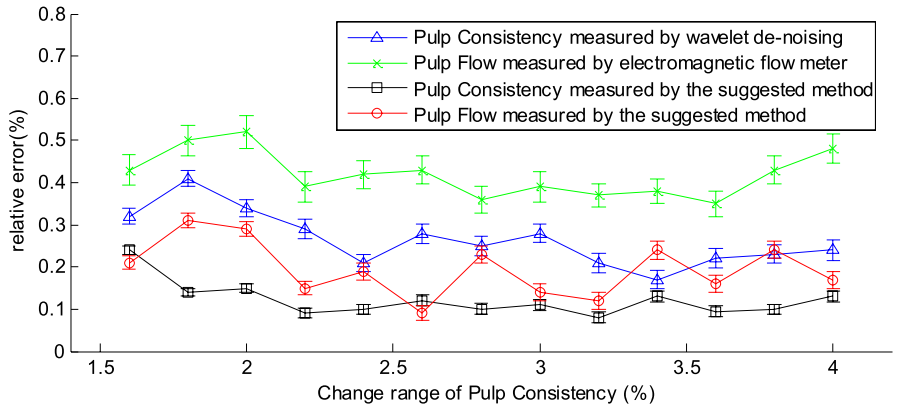

(a)

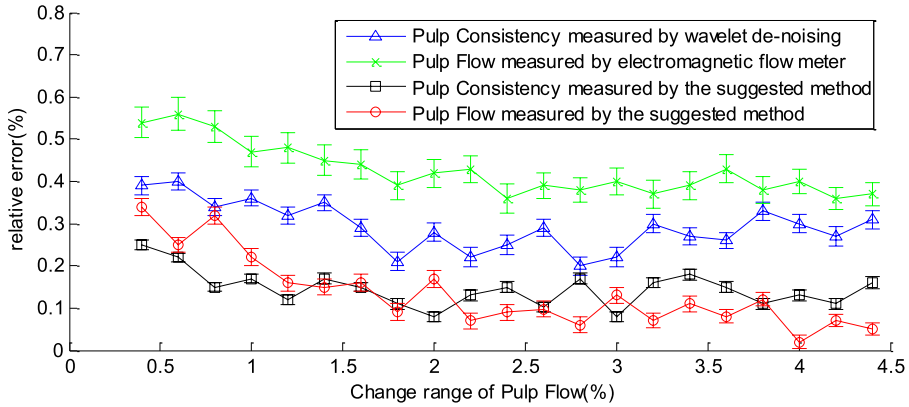

(b)

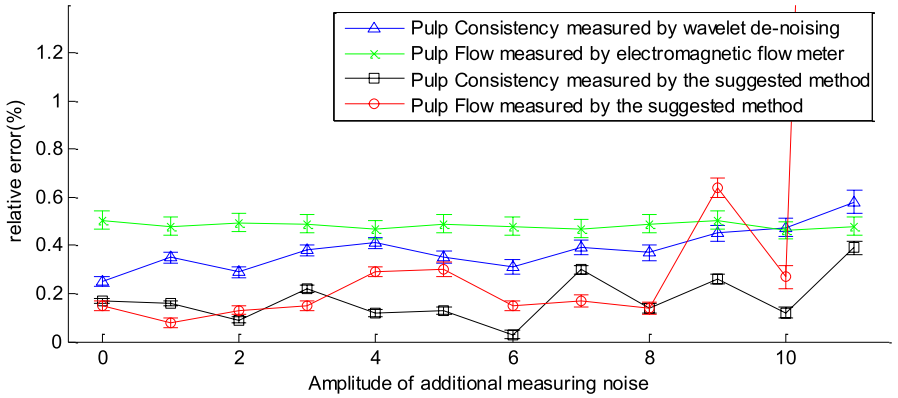

(c)

Figure 11. The applicability experimental results of the proposed integrated measurement method. (a) Applicability to the change in pulp consistency. (b) Applicability to the change in pulp flow. (c) Applicability to the change in noise amplitude.

Table 3. A comparison of pulp flow measurement.

	Cross-correlation method		Electromagnetic flow meter		The suggested method	
Experimental times	Measurement (m s^{-1})	Relative error (%)	Measurement (m s^{-1})	Relative error (%)	Measurement (m s^{-1})	Relative error (%)
1	2.271	0.00	2.269	0.09	2.270	0.04
2	1.518	0.00	1.516	0.13	1. 520	0.13
3	1.336	0.00	1.339	0.22	1.338	0.15
4	0.968	0.00	0.965	0.31	0.970	0.20
5	0.647	0.00	0.650	0.46	0.649	0.31
…	…	…	…	…	…	…
43	0.592	0.00	0.595	0.51	**0.594**	**0.34**
…	…	…	…	…	…	…
45	0.523	0.00	**0.527**	**0.76**	0.524	0.19
…	…	…	…	…	…	…
Maximum error				**0.76**		**0.34**

By analyzing the experimental results, some conclusions can be drawn as follows:

(1) The suggested method is applicable to various types of pulps.
The experimental results show that the suggested method can measure various types of pulps in the papermaking industries and the measuring accuracy has little differences.

(2) The suggested method is insensitive to the pulp consistency change.
As seen from figure 11(a), the influence of pulp consistency change is not obvious in the suggested method. The measuring accuracy of the pulp consistency decreases slightly only at the low concentration.

(3) The suggested method is applicable to the pulp flow varied over a large range.
It can be seen from figure 11(b) that the measuring accuracy of the pulp flow presents a downward trend accompanied with the decreasing flow velocity, but the flow measurement remains certainly accurate on the whole. The measuring accuracy of the pulp consistency is not affected by the flow velocity change.

(4) The suggested method has a strong anti-noise ability.
Figure 11(c) shows that the measuring accuracy of the pulp consistency and pulp flow both present a downward trend with the increasing amplitude of noise. On the whole, the suggested method can oppose the influences of strong amplitude noise, and has better anti-noise ability.

(5) The suggested method shows strong adaptability by utilizing sparse decomposition.
Sparse decomposition is utilized in the suggested method. Sparse atoms of various types and scales are constructed automatically, and the real-time pulp consistency curve is fitted accurately by means of atomic function.
Considering that consistency inherent noises are different in various types of pulps, sparse atoms of various types and scales are constructed in accordance with various pulps. For example, sparse atoms constructed for the mechanical wood pulp at the 2.5% concentration are the Morlet atom at two scales and the Gauss atom at three scales, but the sparse atoms constructed for the sulphate bamboo pulp almost at the same concentration are the Meyer atom at four scales and Mexican Hat atom at two scales. And the pulp consistency change at finite-amplitude does not cause a change in the atom components of the sparse decomposition, but causes a change in the amplitude of the atomic function. Atoms at certain scales may appear or disappear when the pulp concentration changes to a certain extent. Furthermore, pulp flow change just causes a change in the sparse atom scale. And the measurement noise is not affected by factors such as pulp types, pulp consistency and pulp flow. Therefore, the corresponding sparse atoms without scale properties are relatively stable in composition.

(6) The measuring accuracy and measuring stability of the suggested method are higher than traditional measurement methods for pulp consistency and pulp flow, under the various changing conditions.

In a word, the suggested method has strong adaptability, and its feasibility is further verified.

5. Conclusion

We have proposed an integrated measurement method for pulp consistency and pulp flow, based on an original mechanical consistency sensor without adding any hardware. According to the conclusion that the measuring accuracy of the pulp consistency can be affected by two main factors, including the noise components in the pulp consistency signal and the change in flow velocity, two atom dictionaries that have scale properties and scale-free properties are established. Sparse decomposition is conducted on the pulp consistency signal by the atoms from the former atom dictionary, and then noise components that contain flow-velocity information are extracted to calculate flow velocity. The noise is also eliminated using sparse representation. Meanwhile, the noise component without flow-velocity information is separated and eliminated by carrying out sparse decomposition of the pulp consistency signal

with the atoms from the latter atom dictionary. Finally, the calculated pulp flow velocity is employed to compensate the consistency measured value in order to acquire pulp flow velocity and consistency with high precision. The corresponding tests show that the measuring accuracy of the suggested method is higher than current methods, and it has strong applicability.

Acknowledgments

This work was supported by grants from Key Technologies R & D Program of Shaanxi Technology Committee (Grant No. 2016GY-005), the Specialized Research Program of Shaanxi Provincial Department of Education (Grant No. 16JK1105), the Science and Technology Planning Project of Xianyang City (Grant No. 2017K02-06) and the Key Research and Development Program of Shaanxi Province in 2019 (Grant No. 2019GY-090).

ORCID iDs

Xingzhi Tian https://orcid.org/0000-0002-6975-472X

References

[1] Zhou Q 2010 Soft measurement of pulp suspension flow velocity based on wavelet transform *Can. J. Chem. Eng.* **88** 81
[2] Pithon M M *et al* 2015 Intrusive force and pulp flow measurement *Am. J. Orthod.* **148** 891
[3] Stelian C 2015 Application of Manning's formula for estimation of liquid metal levels in electromagnetic flow measurements *Metall. Mater. Trans.* B **46** 449
[4] Xu H J and Aidun C K 2005 Characteristics of fiber suspension flow in a rectangular channel *Int. J. Multiphase Flow* **31** 318
[5] Arola D F *et al* 1998 NMR imaging of pulp suspension flowing through an abrupt pipe expansion *Aiche J.* **44** 2597
[6] Islek A A *et al* 2004 The impact of turbulence and swirl on the flow in the tube bank part of a paper mill headbox *2004 TAPPI Paper Summit - Spring Technical and International Environmental Conf.* pp 417–28
[7] Zhou Q, Han J Q and Wang Y 2005 New approach to measure pulp flow based on cross-correlation theory *China Pulp Pap.* **24** 29
[8] Lu G Q, Fu N C and Zheng Z S 2000 A new method for on-line measuring the concentration of pulp *Acta Metrologica Sinica* **21** 74
[9] Xia C K and Su C L 2015 Reconstruction of electrical capacitance tomography images based on fast linearized alternating direction method of multipliers for two-phase flow system *Chin. J. Chem. Eng.* **24** 597
[10] Wang C, Xu C M, Sun S R and Yue J Q 2013 Effects of ultrasonic treatment on poplar APMP fiber *Pap. Pap. Making* **32** 16
[11] Xiao H B and Chen G 2009 An experimental research on particle size and volume concentration based on light scattering *J. Appl. Opt.* **30** 635
[12] Zhao C 2012 Research on the flow velocity compensation of the static-blade pulp consistency transmitter *Comput. Digit. Eng.* **40** 115
[13] Peng F Q 2010 Sparse signal decomposition method based on multi-scale chirplet and its application to bearing fault diagnosis *Chin. J. Mech. Eng.* **46** 549
[14] Donoho D L and Elad M 2003 Optimally sparse representation in general (nonorthogonal) dictionaries via l1 minimization *Proc. Natl Acad. Sci. USA* **100** 2197
[15] Xie T, Ghiaasiaan S M and Karrila S 2003 Flow regimes and gas holdup in paper pulp–water–gas three-phase slurry flow *Chem. Eng. Sci.* **58** 1417
[16] Barutcigil C *et al* 2012 Micro-tensile bond strength of adhesives to pulp chamber dentin after irrigation with ethylenediaminetetraacetic acid *J. Conservat. Dent.* **15** 242
[17] Zhou Q and Han J Q 2008 Research on improving consistency measuring precision of pulp by dynamics method *Trans. China Pulp Pap.* **23** 100
[18] Huhtanen J P and Karvinen R 2005 Interaction of non-Newtonian fluid dynamics and turbulence on the behavior of pulp suspension flows *Annu. Trans. Nord. Rheol. Soc.* **13** 177
[19] Fitzgerald W J *et al* 1998 Nonlinear and nonstationary signal processing *IEEE Conf. on Colloquium on Non-Linear Signal and Image Processing* (https://doi.org/10.1049/ic:19980449)
[20] Serulle Y *et al* 2015 Diffusional kurtosis imaging in hydrocephalus *Magn. Reson. Imaging* **33** 531–6
[21] Opfer R *et al* 2016 Atlas based brain volumetry: How to distinguish regional volume changes due to biological or physiological effects from inherent noise of the methodology *Magn. Reson. Imaging.* **34** 455
[22] Ma L X, Yang J J and Nie J C 2009 Doppler effect of mechanical waves and light *Lat. Am. J. Phys. Educ.* **3** 550
[23] Aharon M, Elad M and Bruckstein A 2006 K-SVD: An algorithm for designing overcomplete dictionaries for sparse representation *IEEE Trans. Signal Process.* **54** 4311
[24] Xu J, Chang Z G and Zhao X Q 2013 Discriminate dictionary training algorithm based on adaptive steepest descent *Comput. Eng.* **39** 225
[25] Feng L *et al* 2012 Dual dictionary sparse restoration of blurred images *Opt. Precis. Eng.* **19** 1982